ACS Sustainable Chemistry & Engineering

Perspective

pubs.acs.org/journal/ascecg

Titanium Dioxide Microsphere-Derived Materials for Solar Fuel Hydrogen Generation

Kai Yan*,† and Guosheng Wu*,‡

†School of Engineering, Brown University, 182 Hope Street, Providence, Rhode Island 02912, United States

‡Department of Chemistry, Lakehead University, 955 Oliver Road, Thunder Bay, Ontario P7B 5E1, Canada

ABSTRACT: Hydrogen fuel is an excellent energy carrier for the development of a low carbon emission economy that has the potential to solve the energy and environmental problems in the future. Photocatalytic H_2 generation has received significant growth over the past few decades. Due to their unique properties, TiO_2 microspheres have attracted much attention to be utilized in the photocatalytic H_2 generation from water splitting. These microspheres-derived photocatalysts are known to offer the advantages of large surface area, tunable pore sizes, better allowing light absorption, efficient carrier separation, excellent electronic and optical properties, and high durability. Over the past few decades, significant research efforts have been allocated to the design of TiO_2 microspheres with desired functionality for efficient H_2 generation. This perspective will concentrate on recent advances in the synthesis of TiO_2 microsphere-derived photocatalysts and their applications for efficient solar fuel H_2 evolution from water splitting. Advanced strategies for the fabrication of TiO_2 microsphere-based materials have been critically reviewed. The up-to-date developments of technologies applied to TiO_2 microsphere-based materials for photocatalytic H_2 evolution are compared and commented. Current challenges and future perspectives for solar fuel H_2 generation will be also highlighted and discussed.

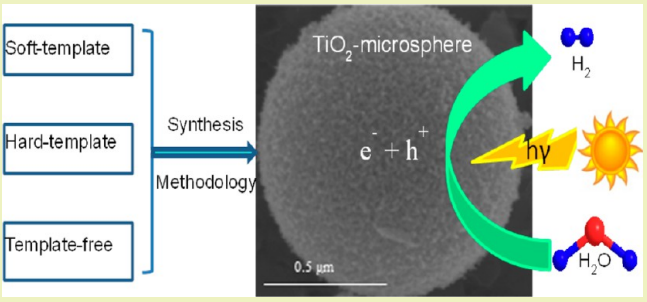

KEYWORDS: *Titanium dioxide, Microsphere, Synthesis, Template, Photocatalytic, Hydrogen evolution*

INTRODUCTION

Nowadays, with the rapid depletion of fossil fuels (e.g., coal, natural gas, and petroleum oil) and the political concerns on environmental issues, the development of renewable energies based on sustainable energy sources for the long-term is in high demand.[1] It has spurred a number of efforts in exploring novel methods for developing renewable energy technologies. Over the past few decades, it has been demonstrated that the conversion of solar energy into chemical energy in the form of solar fuels (e.g., H_2, methanol, methane) is one of the most promising solutions to reduce our high dependence on the diminishing fossil resources to solve the energy and environmental problems in the future.[2−6]

H_2 is an excellent energy carrier for the development of a low carbon emission economy. Although H_2 may associate with the safe transportation issue, it has several overwhelming advantages:[4,6−11] (1) no harmful emissions, the biggest advantage of the utilization of H_2 energy is that almost no harmful byproducts are left when it is burned; (2) environment benignity, H_2 is also nontoxic, which makes it a rarity among fuel sources; (3) efficient fuel, H_2 energy is much more efficient fuel source than traditional sources of energy and produces more energy per pound of fuel; (4) wide resources, H_2 is the most abundant element that can be obtained from a broad range of substances (e.g., alcohol, biomass); (5) platform chemical, H_2 is also an important chemical reagent in the chemical industry. To develop the H_2 economy, extensive research has been carried out on the photocatalytic or photoelectrochemical (PEC) splitting of water into H_2 as fuel since the first report on TiO_2 electrode by Honda and Fujishima.[12]

One of the earliest studied *n*-type semiconductor photocatalysts, TiO_2, has been widely used in our previous works and other groups' studies in environmental purification,[13−16] H_2 production,[11,17−19] photosynthesis,[20−23] CO_2 reduction,[4,24,25] methanol fuel cell,[26] organic synthesis,[27] solar cells,[3,28] etc. Due to its unique and attractive properties (e.g., cheap, stable, nontoxic, and environmentally friendly), TiO_2 has been demonstrated as an ideal model of semiconductor photocatalyst for the photocatalytic fuel generation, especially for H_2 production.[29−31] Different morphologies of TiO_2 such as nanoparticles, nanowires, and nanotubes have been fabricated. To extend the absorption edge to the visible light range, doped or modified TiO_2-based materials were also developed.

It is well demonstrated that the crystal structure of synthesized TiO_2 powders will crucially influence their photocatalytic performances.[2,5,12,13] TiO_2 can be present in various microcrystalline structures, of which the most relevant are rutile, anatase, and brookite, as shown in Figure 1. The fundamental structural unit derived from TiO_6 octahedron that

Received: February 27, 2015
Revised: April 1, 2015
Published: April 21, 2015

DOI: 10.1021/acssuschemeng.5b00154
ACS Sustainable Chem. Eng. 2015, 3, 779−791

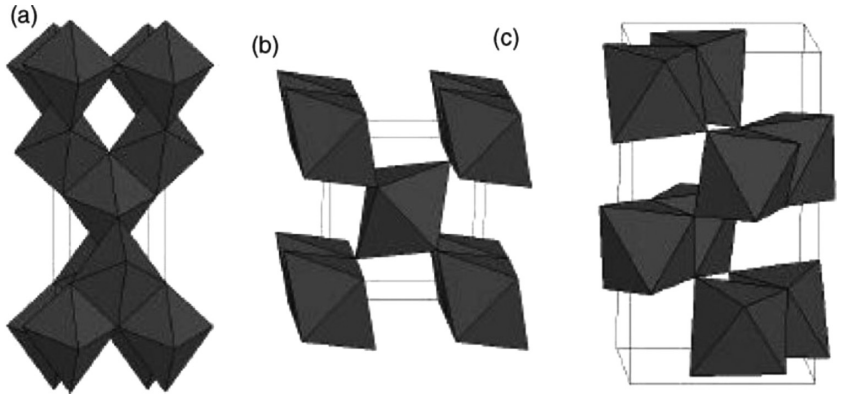

Figure 1. Connectivity of TiO_6^{2-} octahedral units in (a) anatase, (b) rutile, and (c) brookite. Reprinted with permission.[28] Copyright 2004, Elsevier.

Table 1. Physical Properties of Different TiO_2 Crystal Phases[1,28,39]

	rutile	anatase	brookite
crystal structure	tetragonal	tetragonal	orthorthombic
lattice constant (Å)	a = 4.5936	a = 3.784	a = 9.184
	c = 2.9587	c = 9.515	b = 5.447
			c = 5.145
space group	$P4_2/mnm$	$I4_1/amd$	$Pbca$
TiO_2 molecule/cell	2	4	8
volume/molecule (Å^3)	31.216	34.061	32.172
density (g/cm^3)	4.13	3.79	3.99
Ti−O bond length (Å)	1.949−1.980	1.937−1.965	1.87−2.04
O−Ti−O bond angle	81.2−90.0°	77.7−92.6°	81.2−90°

Table 2. Typical Works for the Synthesis of Nanostructured TiO_2 Microspheres

no.	titanium resources	methods	surfactant and/or additives	crystal phase	ref
1	titanium(IV) ethoxide	soft template	poly(acrylic acid), diethylene glycol, alcohol	amorphous	45
2	tetrabutyl titanate	soft template	polyethylene glycol, HCl, $CO(NH_2)_2$, glacial acetic acid	A	46
3	titanium(IV) isopropoxide	soft template	poly(acrylic acid), diethylene glycol, alcohol	amorphous	45
4	titanium butoxide	soft template	formamide, octadecene sodium dodecyl sulfate	A	47
5	titanium *n*-butoxide	soft template	ethanol, glycine	A	48
6	titanium tetrafluoride	soft template	sucrose	A	49
7	titanium chloride	soft template	ethanol, P123, urea	A	19
8	titanium chloride	soft template	ethanol, CTAB, urea	A	19
9	tetrabutylorthotitanate	template-free	KCl, NH_4F	A	50
10	titanium butoxide	hard template	SiO_2 nanosphere, oleylamine, benzyl ether	A	51
11	titanium isopropoxide	hard template	poly(methyl methacrylate), HCl	A	52
12	titanium tetraisopropoxide	hard template	polystyrene, poly(vinylpyrrolidone), water, ethanol	A	53
13	tetrabutyl titanate	hard template	polystyrene, sulfuric acid, ethanol, water	A	54
14	potassium titanium oxalate	template-free	H_2O_2, HCl	R	55
15	titanium chloride	template-free	alcohol, acetone	A	56
16	titanium(III) chloride	template-free	butanol, HCl	R or R+A	57
17	titanium chloride	template-free	HCl, Na_2SO_4	R or R+A	58
18	titanium chloride	template-free	benzyl alcohol	A	59
19	titanium butoxide	template-free		amorphous	60
20	titanium butoxide	template-free	ethanol, H_2SO_4	A or A+R	61
21	titanium sulfate	template-free	ammonium fluoride, ethanol	A	62
22	titanium(IV) oxysulfate	template-free	glycerol, ethyl ether	A	63

Note: R, rutile; A, anatase; P123, poly(ethylene glycol)-*block*-poly(propylene glycol)-*block*-poly(ethylene glycol); CTAB, hexadecyltrimethylammonium bromide.

has different modes of arrangement is depicted in Figure 1. The unit cell, crystal structure, and properties of these types of TiO_2 structures can be found in Table 1.

Structures based on microspheres are known to offer the advantages of better allowing light absorption, the simultaneous efficient carrier separation and collection in the nanometer scale radial direction, and high durability.[5,13,19] Over the past few decades, significant research efforts have been allocated to the design of nanostructured TiO_2 microspheres with specific functionality. They share certain common characteristics with

DOI: 10.1021/acssuschemeng.5b00154
ACS Sustainable Chem. Eng. 2015, 3, 779−791

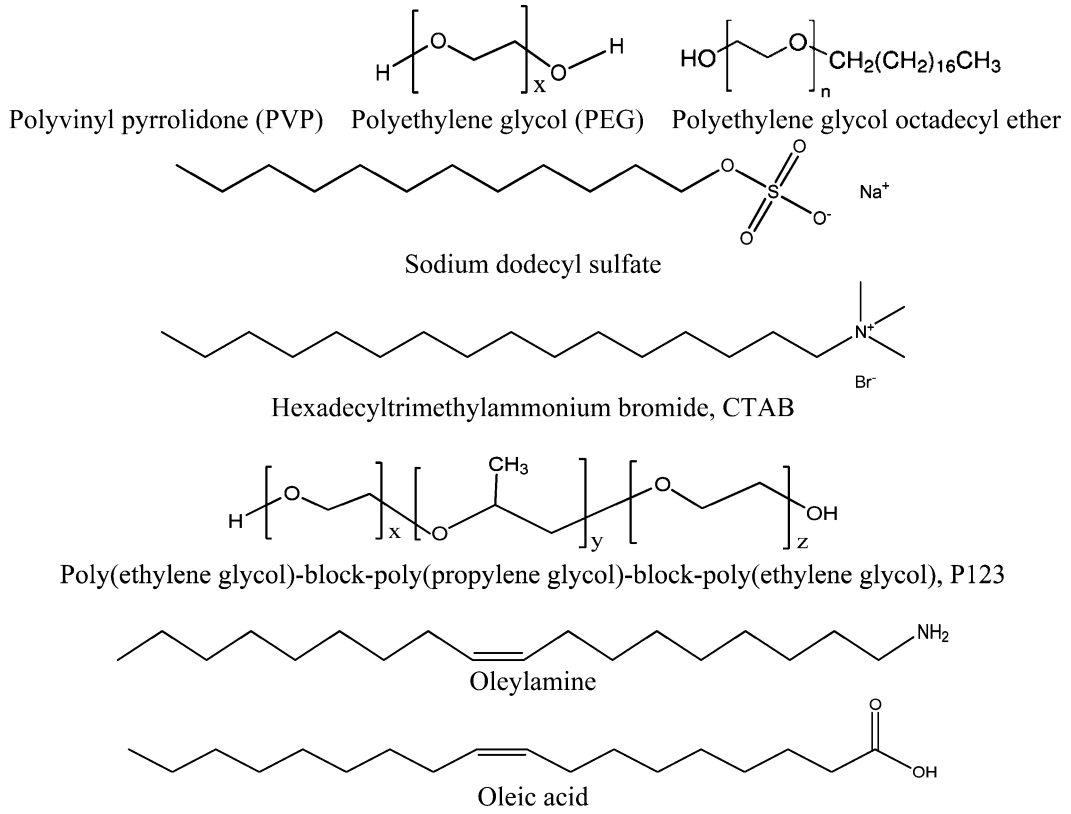

Figure 2. Some commonly utilized surfactants in soft templating methods.

TiO_2 nanoparticles and thin films, such as stable crystal structure and quantum confinement effects. However, geometrically they offer unique properties that are difficult to achieve in the latter two categories. These fabricated TiO_2 microspheres-derived photocatalysts present good crystallinity, large specific surface area, and tunable pore volume and pore size, with these properties increasing the size of the accessible surface area and the rate of mass transfer for visible or UV–visible light adsorption.[32] These structural features increase the light-harvesting capabilities of these materials because they enhance light use by allowing as much light as possible to access the interior and reduce the recombination of electrons and holes. Their light-harvesting capability makes them good candidates for use in photocatalysis with the advantages of high photocatalytic activity and good durability. The good chemical and thermal stability would render them to be recycled for use over several runs. Due to their unique material properties (e.g., large surface area, good chemical and thermal stability, and excellent electronic and optical properties), TiO_2 microsphere-derived materials have received significant growth and wide applications in photocatalysis, solar cells, lithium-ion batteries, catalyst supports, and heterogeneous catalysis.[14,33−38] Several reviews on TiO_2 materials and photocatalytic H_2 generation have been published so far.[1,2,37−39] However, no review on TiO_2 microsphere-derived photocatalysts has been reported. In this perspective, we will concentrate on the recent advances in the synthesis of nanostructured TiO_2 microsphere-derived photocatalysts and their applications for efficient solar fuel H_2 generation.

METHODS FOR FABRICATION OF TIO_2 MICROSPHERE-DERIVED MATERIALS

The photoactivity of TiO_2 microsphere-derived materials has been shown to be dependent on several key properties: crystal structure, surface area, porous structure, uncoordinated surface sites, defects in the lattice, and degree of crystallinity.[40−42] Morphology control of TiO_2 microsphere-derived materials through synthesis has allowed for the improvement and fine-tuning of many of these properties. The anatase phase is typically considered more favorable, as it has a higher reduction potential and a slower rate of recombination of electron–hole pairs.[41,42] A comprehensive overview of synthetic approaches for the fabrication of TiO_2-microsphere derived hollow structures will be presented. These studied strategies can be generally divided into three types: (1) soft templating synthesis, (2) hard templating synthesis, and (3) template-free methods. TiO_2 microspheres-derived materials are typically prepared from a titanium alkoxide (e.g., titanium tetraisopropoxide, titanium chloride).[43,44] To compare better the synthesis precursor, synthesis conditions and the resulted morphology are depicted in Table 2.

Soft Template Synthesis. A template usually works as the structure directing agent (SDA) in the fabrication of porous materials. The templating routes employing cationic, nonionic, and anionic surfactants as the SDA have given rise to a variety of mesoporous structures. The utilization of the surfactant is to reduce the surface tension or interfacial tension between two liquids. The structure of the surfactant often has a hydrophobic (nonpolar) hydrocarbon "tail" and a hydrophilic (polar) "head" group in a molecule. These molecules have high molecular weight and are easy to aggregate in solvent to form the self-assembled micelle.[64,65]

The soft template method is probably the most common and effective method to synthesize TiO_2 microspheres.[43,48,66] It is relatively easy to operate and control the synthesis parameters with high yields of products. Another advantage is that the soft template is easy to remove either by extraction or calcination. Over the past decades, soft templates have attracted the greatest attention and significant progress has been made. Figure 2 depicts typical soft templates utilized in the

DOI: 10.1021/acssuschemeng.5b00154
ACS Sustainable Chem. Eng. 2015, 3, 779–791

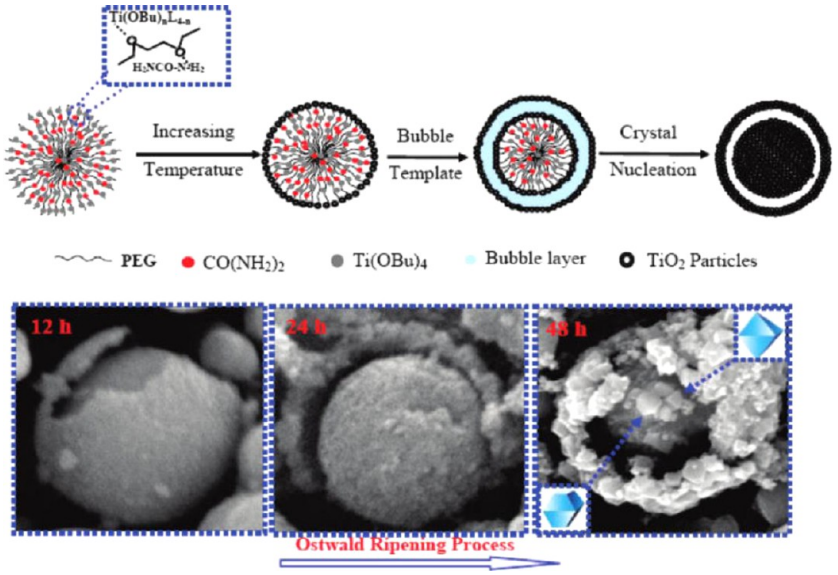

Figure 3. Schematic representation of the formation of core−shell structured titanium dioxide hollow spheres. Below is the morphology evolution of core−shell TiO_2 microspheres with the hydrothermal time. Reproduced with permission.[46] Copyright 2010, American Chemical Society.

synthesis of TiO_2 microspheres. In the soft templating route, usually there are three steps to form a porous solid. In the first step, the surfactant (e.g., block copolymers) will go through self-assembly and form micelles. By means of self-assembly, either concentration-driven or induced by external promoter such as temperature, the surfactant can undergo microphase segregation to give various morphologies (micelles, vesicles, rods, and tubes) in solution. Subsequent organization of the inorganic precursor over the surfactant via self-assembly occurs, to form a stable inorganic−organic hybrid in the second step. The last step is the removal of organic template, to result in porous TiO_2 microspheres. Calcination in aerial atmosphere is the most familiar and simple method to remove the organic template completely, which is also widely for the synthesis of mesoporous silica and metal oxides.[67−70] The exact calcination temperatures required for removing templates are different, which are often determined by thermogravimetric analysis (TG) and differential thermal analysis (DTA).

By virtue of a soft template and well-tuning synthesis parameters, a well-crystallized TiO_2 microsphere with high specific surface area and large pore volume and pore size can be successfully fabricated, and these properties would enhance the accessibility and the rate of mass transfer for visible or UV−visible light adsorption. Cui et al.[46] reported the mesoporous core−shell structured TiO_2 microspheres with a large surface area of 113.8 m^2/g and an average pore size of 5.78 nm, which were prepared in the presence of soft template polyethylene glycol (PEG, MW of 2000). The authors found that the hydrothermal reaction time presented a crucial influence on the morphology control. They concluded that the shell morphology and the core size of core−shell TiO_2 spheres can be tuned by controlling the hydrothermal time through the Ostwald ripening process, as shown in Figure 3. With a short hydrothermal reaction time (12 h), crystallite nanoparticles of TiO_2 microspheres were small and gave a smooth surface morphology. The crystallite nanoparticles grow bigger and brought a rougher surface morphology with increasing the hydrothermal time to 24 and 48 h. At 48 h, a dramatic morphology change occurred with the transition from solid primary spherical particles to well-faceted TiO_2 nanoparticles.

Jiao et al.[47] employed sodium dodecyl sulfate as the template to synthesize TiO_2 hollow spheres consisting of {116} plane-oriented nanocrystallites, where titanium butoxide was used as the precursor, formamide and octadecene served as water phase and oil phase, and the additive H_2O was used for titanium butoxide hydrolysis. The interior structure was examined by transmission electron microscopy (TEM), as shown in Figure 4. A TEM image revealed an interior

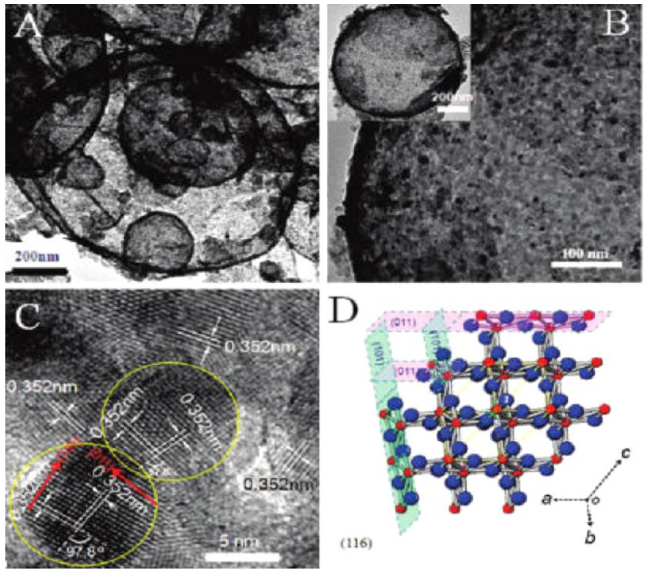

Figure 4. TEM (A, B) and HR-TEM (C) images of TiO_2 hollow spheres, and (D) the crystal structure diagram along TiO_2 {116} planes. The inset in panel B is a hollow sphere arbitrarily selected for local sited HR-TEM. Red spheres and blue spheres in panel D present Ti atoms and O atoms. Reproduced with permission.[47] Copyright 2011, American Chemical Society.

enclosed by a thin shell of TiO_2 and different diameters of the TiO_2 hollow spheres were observed (Figure 4A). An individual sphere was selected to show the hollow interior and the clear shell (inset of Figure 4B). The shell thickness was ~10 nm and consisted of large numbers of crystallites (5−10 nm) with lots of intercrystallite nanopores uniformly dispersed (Figure 4B), revealing a mesoporous structure with a large surface area. With high resolution (HR)-TEM, clear boundaries and crystal lattice fringes of crystallites with diameters of 5−10 nm were observed, which matched well with the anatse TiO_2 crystal structure. A more intuitive understanding of the {116} orientation is proposed in Figure 4D. The core−shell structure of TiO_2 was successfully fabricated, and the homogeneous dispersion may require further careful control.

Hard Template Synthesis. Due to some metal oxides that cannot be synthesized by soft template methods, a hard template has been

DOI: 10.1021/acssuschemeng.5b00154
ACS Sustainable Chem. Eng. 2015, 3, 779−791

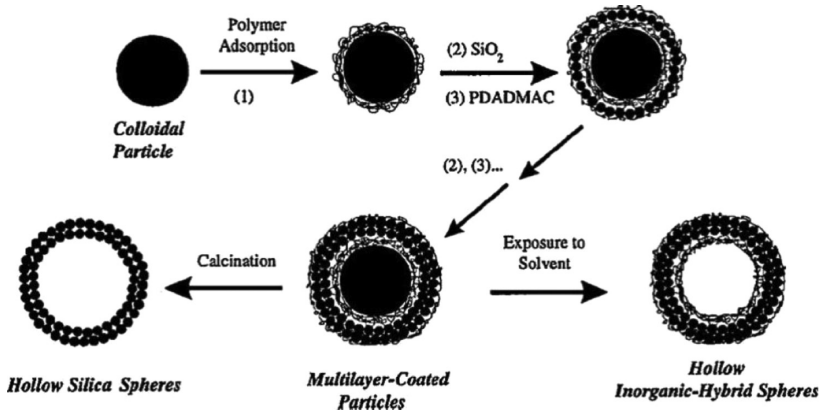

Figure 5. Schematic illustration of procedures for preparing inorganic and hybrid hollow spheres based on PS colloidal templates. Reproduced with permission.[72] Copyright 1998, AAAS.

developed and considered as an attractive route to produce highly crystalline mesoporous metal oxides.[43,66,71] Highly crystalline mesoporous metal oxide with well-defined crystal structures and facets can not only offer high surface areas and fast carrier transport across the crystal framework but also provide a pathway for tailoring crystal surface, changing the selectivity and reactivity.[71]

A hard template is often a solid material such as SBA-15, SBA-16, FDU-12, or KIT-6, which is often filled with carbon or coating silica layers inside mesopores of the amorphous precursor.[73,74] After crystallization by calcination, the carbon or silica layers can be removed by calcination in air or treated with an alkaline (e.g., 1 M KOH) solution. This method has been widely used for producing crystalline mesoporous metal oxides materials.[69] Overall, hard template synthesis can be divided into four major steps, as illustrated in Figure 5: (1) the fabrication of hard templates, (2) the functionalization/modification of template surface, (3) the templates hybrid with the target metal precursors, and (4) selective removal of templates to obtain microsphere structures. The most commonly employed hard templates include monodisperse silica particles, mesoporous carbon, and polymer latex colloids. The utilization of these templates was benefited from their narrow size distribution, and was relatively easy to be fabricated in a large amount. In general, step 3 was the most crucial and was commonly considered as the most challenging because it needed special attention to the fabrication of the shell layer with controllable size. Step 4 was the simplest, in principle. It typically entailed selective etching of the template in appropriate solvents or calcination of the template at high temperatures.

Kondo et al.[53] reported the synthesis of TiO_2 hollow spheres by the hydrolysis of titanium tetraisopropoxide in which polystyrene was used as a hard template and was initially coated with the titanium species. Polystyrene surfactants were removed through the calcination process, and the titanium species converted to TiO_2, which resulted in the formation of TiO_2 hollow spheres. The resulting TiO_2 hollow spheres possessed a large specific surface area and the potential for multiple diffractions and reflections of light, providing the sphere with properties that are advantageous for photocatalytic decomposition. These advantages were clearly demonstrated by the superior photocatalytic decomposition rate of 2-propanol using the TiO_2 hollow spheres compared with the rate achieved using commercially available TiO_2 particles (P25). Lu and co-workers have developed the synthesis of hollow spheres with a double-shelled complex structure by using commercial polymer hollow spheres as templates. They described an interesting approach to prepare inorganic hollow spheres via preferential adsorption of inorganic precursors into the sulfonated shell layer of PS templates.[54,75] The core/shell PS templates were obtained by an inward sulfonation of PS particles with the concentrated sulfuric acid. The sulfonation process would produce hydrophilic shells with sulfonic acid groups randomly attached to PS chains.

Recently, Dinh et al.[51] reported the synthesis of a three-dimensional ordered assembly of thin-shell Au/TiO_2 hollow nanospheres from a SiO_2 microsphere template. In the first step, the SiO_2 microsphere was initially coated with titanate nanodisks, then a gold precursor (H_4AuCl_4) was loaded on it. After self-assembly, the resulted samples were calcinated to obtain the $Au/TiO_2/SiO_2$ nanocomposite. The hard template of SiO_2 was finally removed by concentrated NaOH. The designed materials exhibit not only exceedingly high surface area but also photonic behavior originating from periodic macroscopic voids from both the inside and the outside of hollow spheres that have very thin shells. This strategy is considered as very suitable for controlling the shell thickness and has potential in scale-up application.

Over the past several decades, great developments have also been made in the synthesis and application of TiO_2 microsphere-derived nanocomposites using the hard template method.[42,76−78] Song et al. employed the hard template (polystyrene) method to successfully fabricate well-defined nitrogen doped, hollow SiO_2/TiO_2 hybrid spheres,[76] where triethylamine was used as the nitrogen source. The synthetic approach is proposed in Figure 6. The first step was to

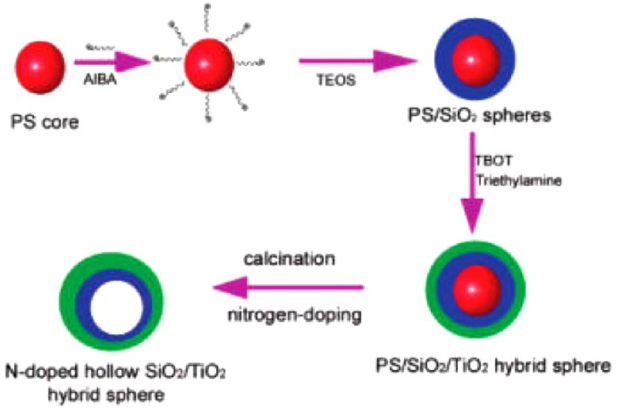

Figure 6. Preparation of N-doped, hollow SiO_2/TiO_2 hybrid spheres. Reprinted with permission.[76] Copyright 2007, American Chemical Society.

synthesize polystyrene (PS)/silica microspheres, and then triethylamine was used to treat PS/silica microspheres and insert the nitrogen resource inside the microsphere. The last step was the elimination of the PS core, nitrogen-doping process, and crystallization of amorphous TiO_2 in the calcination process to acquire the final hollow structure. XPS analysis in their study displayed the anatase TiO_2 shell was composed of N−Ti−O and Ti−N−O.

In general, templating methods have been widely employed to generate multiple hollow structures.[43,80,81] A surfactant or polymer was often added to provide a porous structure in the presence of an acid or

DOI: 10.1021/acssuschemeng.5b00154
ACS Sustainable Chem. Eng. 2015, 3, 779−791

salt to promote the synthesis.[82,83] During the past few decades, a large number of investigations have focused on interactions between surfactants and titanium species in the realization of specific morphology control.[84] The conclusion has been reached that the surfactant−titanium precursors spontaneously organize through the interactive matching of organic and inorganic components in the synthesis process. Through the careful control of the self-assembly, titanium condensation rate, and other parameters, it is possible to change the dimensions, crystal structures, and morphologies of the resulted microspheres.[13,32,85,86]

Template-Free Synthesis. Template methods are very effective and versatile for synthesizing a wide array of TiO_2 microspheres, even for other hollow metal oxides structures.[69] However, some clear drawbacks still exist. The high cost and tedious synthetic procedures have impeded scale-up of many of these methods for large scale utilization. Besides, the template-removal step is unavoidable when hard templates are used. It will not only increase the cost but also detrimentally affect the quality (e.g., high impurity levels and inevitable shell collapse) of the fabricated TiO_2 microsphere. The template-free method is more ideal for the controlled preparation of hollow structures in a wide range of sizes. Over the past few decades, many researchers have contributed a lot to this method, as shown in Table 2.

Li et al. reported the preparation of hollow TiO_2 spheres with a sphere-in-sphere structure using a template-free process, and the resulting spheres were found to have high photocatalytic activity,[33] where the multiple scattering and reflections of light within the TiO_2 spheres would extend the light path length. Liu et al.[34] studied the synthesis of hollow TiO_2 microspheres with exposed {001} facets by using a modified fluoride-mediated self-transformation strategy and titanium sulfate as a Ti resource. Ethanol solvent was used to stabilize {001} facets of the resulted anatase polyhedra. Ammonium fluoride (NH_4F) was used as an additive to promote the reaction. The internal structure of the resulting TiO_2 microspheres was examined by SEM (Figure 7). Figure 7a displays a relatively homogeneous dispersion,

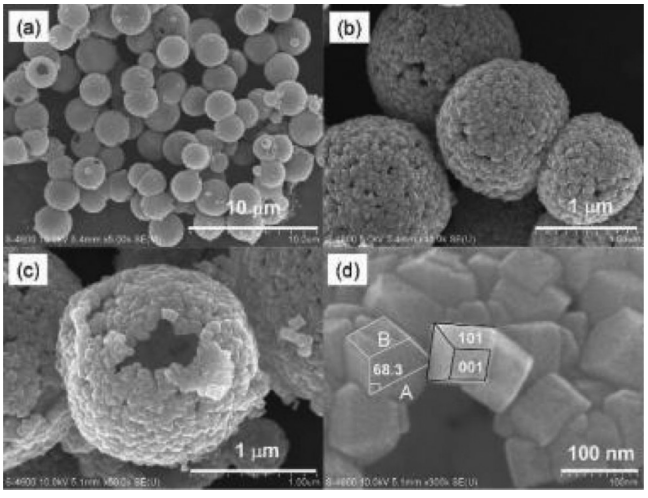

Figure 7. Scanning electron microscopy (SEM) images of the fluoride-mediated TiO_2 samples: (a) overall view of TiO_2 microspheres; (b) image of a few microspheres showing their unique structure consisting of primary TiO_2 nanoparticles; (c) single microsphere showing its hollow nature; (d) portion of the microsphere shell composed of nanosized polyhedra with exposed {001} facets. Reprinted with permission.[62] Copyright 2010, American Chemical Society.

and when zoomed-in (Figure 7b), some microspheres were found to be connected with each other. Searching different areas, we found some broken microspheres indicated the interior void structure (Figure 7c). The surface with exposed {001} facets was observed (Figure 7d). The template-free method is not only successful for the synthesis of the hollow interior structure but also can ideally introduce the dopant inside.

Shang et al.[56] reported that submicrometer-sized anatase TiO_2 microspheres were fabricated through a template-free solvothermal route using titanium(IV) chloride as a raw material and a mixture of alcohols−acetone as the solvent at 220 °C for 12 h. The use of titanium chloride as a precursor needs special attention because it is too easy to be hydrolyzed even under the air environment. It was reported that TiO_2 microsphere with sizes from 400 nm to 1 μm can be obtained by adjusting the ratio of alcohol to acetone in the solvothermal system. TEM and field emission (FE)-SEM images (Figure 8a,b) indicated the presence of uniform hollow structures with

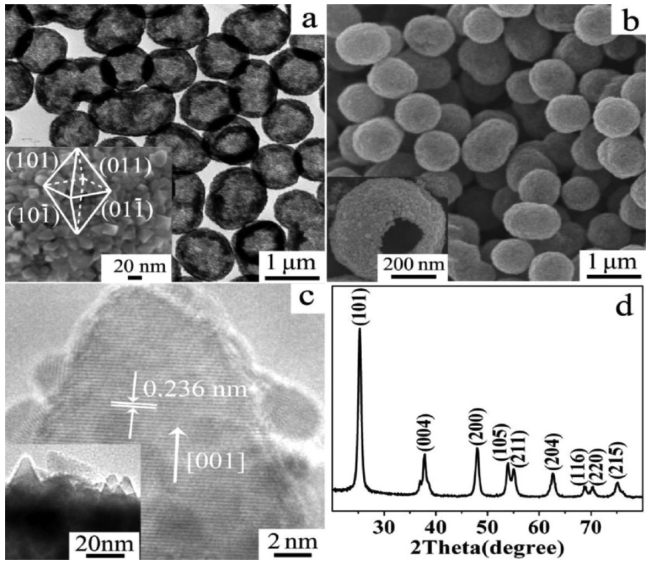

Figure 8. TEM (a), SEM (b), and HR-TEM (c) images, and (d) XRD pattern of the solvothermal product (THS-E). The insets in panels a, b, and c are, respectively, the images of a sphere's surface, a broken hollow sphere, and the local surface of a hollow sphere. Reprinted with permission.[56] Copyright 2012, American Chemical Society.

a wall thickness of 40−60 nm and a diameter of 0.8−1.0 μm. HR-TEM images display that the hollow spheres were randomly aggregated by the TiO_2 nanoparticles of ca. 20 nm (Figure 8c), where the nanoparticles are octahedral double cones with some 3−4 nm particles attached on the surfaces. The interplanar distance of 0.236 nm corresponded to the (004) plane of anatase TiO_2. The X-ray diffraction (XRD) pattern of the solvothermal product (Figure 8d) indicated that all the reflections could be indexed to tetragonal anatase TiO_2 and no peaks of impurities were observed, indicating the anatase phase-pure nature of the product. They further proposed the formation mechanism. In the first step, $TiCl_4$ was considered to be hydrolyzed to form anatase TiO_2 nanoparticles followed by the quick aggregation, the TiO_2 microsphere will be formed through the final step named Ostward ripening. In general, this method is easy to operate, and prone to produce TiO_2 microspheres in a large amount. Following the similar process, TiO_2 microspheres with radially assembled single crystalline TiO_2 nanorods were also successfully fabricated and exhibited high performance in dye-sensitized solar cells.[57]

Kandiel et al.[87] reported the tailorable synthesis of TiO_2 with different structures and found that high quality brookite TiO_2 nanorods could be obtained by the thermal hydrolysis of commercially available aqueous solutions of titanium bis(ammonium lactato)-dihydroxide in the presence of high concentrations of urea (6.0 M), as shown in Figure 9. Low concentrations of urea (0.1 M) would produce mainly anatase microspheres. By the systematic investigation of different parameters, the authors suggested that there was no phase transformation (anatase ↔ brookite) during the synthesis. The ratios between anatase phase and brookite phase can readily be tuned through the control of the urea concentration. This method provides

DOI: 10.1021/acssuschemeng.5b00154
ACS Sustainable Chem. Eng. 2015, 3, 779−791

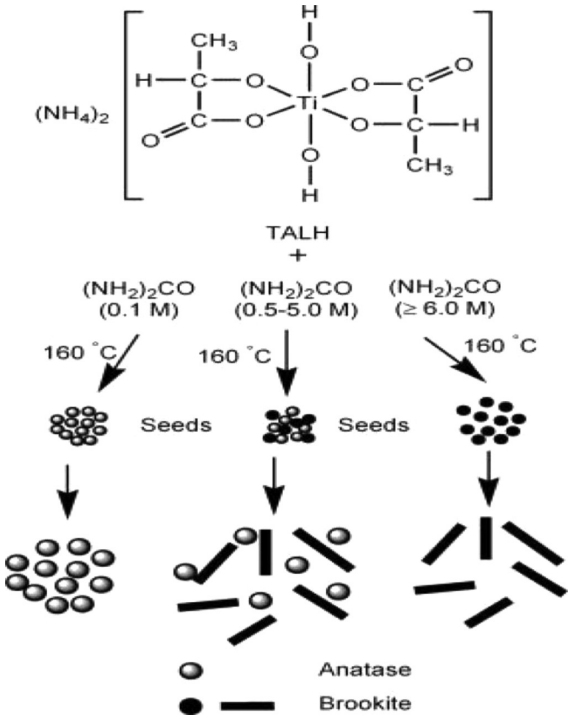

Figure 9. Suggested reaction pathways for the hydrolysis of titanium bis(ammonium lactato)dihydroxide in the presence of varying concentrations of urea to form either anatase particles or brookite rods or mixtures thereof. Reprinted with permission.[87] Copyright 2010, American Chemical Society.

an alternative for the tailorable synthesis of TiO_2 microsphere with tunable phase structure.

Recently, wang et al.[88] reported that the single-crystalline hollow TiO_2 spheres were produced through a simple one-step laser process performed at room temperature. Single-crystalline hollow spheres were successfully produced due to the unique pulsed laser heating. The fabrication process combined mechanic property and chemical route together, as shown in Figure 10. In the first step, abundant voids were created in agglomerates of TiO_2 nanoparticles through high dispersing in liquids (Figure 10a). In the second step (Figure 10b), the TiO_2 congeries absorb laser energy upon pulsed laser irradiation, the liquid layer would be around particles that are not yet melted in the center, and will capture the air inside the agglomerate during its further melting process. Through a mechanism analogous to the Kirkendall effect, the hollow center would be formed (Figure 10c). After numerous pulsed heating cycles, the sphere would grow up by fusion with nearby nanospheres and recrystallize into a single crystalline hollow sphere (Figure 10d). The clear advantages of this process are performed at room temperature, and the size-tailored hollow spheres display tunable light scattering over a wide visible-light range.

PHOTOCATALYTIC H_2 GENERATION ON TIO_2 MICROSPHERE-DERIVED MATERIALS

Hydrogen Evolution Process. Water splitting into H_2 and O_2 needs the standard Gibbs free energy change ΔG_0 of 237 kJ/mol or 1.23 eV, as shown in eq 1:

$$H_2O \rightarrow 1/2O_2 + H_2, \quad \Delta G = +237\ \text{kJ/mol} \tag{1}$$

Thus, the bandgap energy (Eg) of TiO_2 microsphere-derived photocatalysts should be >1.23 eV for water splitting. To use efficiently the visible light, Eg should be lower than 3.0 eV (λ > 400 nm). Efficient H_2 production requires the level of conduction band to be more negative than the reduction potential of H^+/H_2 [0 V vs NHE (normal hydrogen electrode)].

Figure 11 shows a schematic diagram of water splitting into H_2 and O_2 over TiO_2 microsphere semiconductor photo-

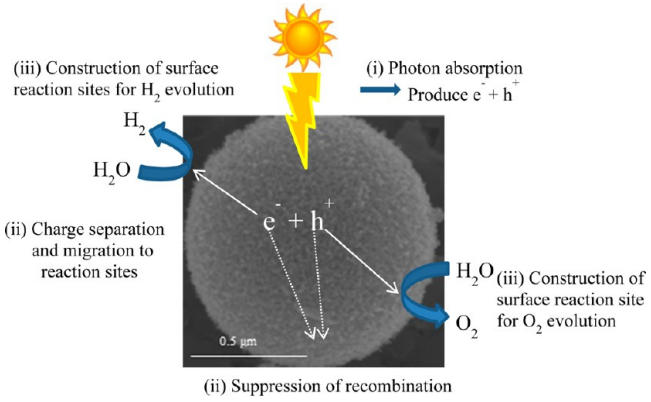

Figure 11. Schematic of different processes of photocatalytic water splitting. SEM image reprinted with permission.[19] Copyright 2014, Elsevier.

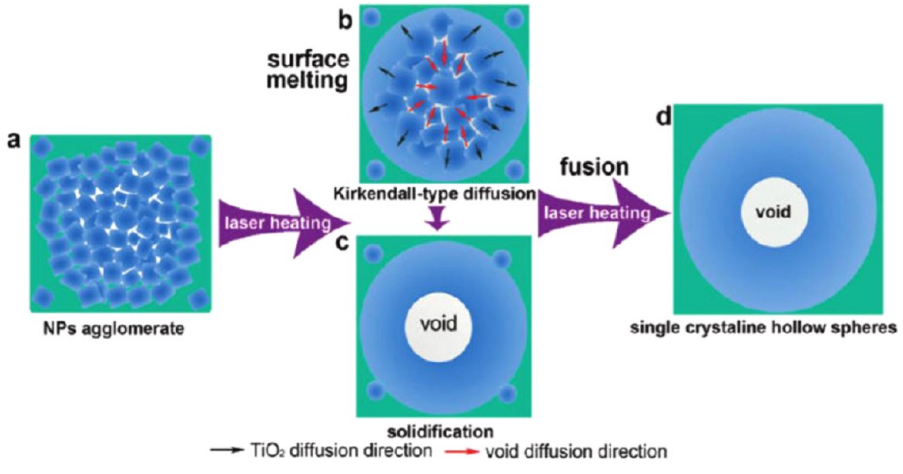

Figure 10. Schematic illustration of single-crystalline TiO_2 hollow sphere formation by bottom-up laser processing range. Reprinted with permission.[88] Copyright 2011, American Chemical Society.

DOI: 10.1021/acssuschemeng.5b00154
ACS Sustainable Chem. Eng. 2015, 3, 779−791

Table 3. Recent Advances of H_2 Evolution on TiO_2 Microsphere-Derived Photocatalysts

no.	catalyst	reaction conditions	irradiation type	H_2 evolution rate	quantum efficiency	refs
1	0.4 wt % Pt-C/TiO_2	80 mL of water, 20 mL of methanol, quartz reactor	500 W Xe lamp, UV−visible light	26.2 μmol h^{-1} g^{-1}	N.D.[a]	99
2	0.6 wt % Pt-C/TiO_2	80 mL of water, 20 mL of methanol quartz reactor	500 W Xe lamp, UV−visible light	24.6 μmol h^{-1} g^{-1}	N.D.	99
3	1 wt % Pt/TiO_2	focused intensity: ~300 mW cm^{-2}, 1 mg catalyst, 3 mL water−methanol	450 W Xe lamp with a cutoff filter (λ > 400 nm)	200 μmol h^{-1} g^{-1}	N.D.	34
4	2 wt % Pt/F-TiO_2	focused intensity: ca. 20 mW/cm^2, 20 mL ethanol and 60 mL water	350 W Xe arc lamp, UV−visible	16.7 mmol h^{-1} g^{-1}	N.D.	100
5	0.23 mol $Ni(OH)_2$/TiO_2	Pyrex flask, focused intensity: ~ 80 mW/cm^2, 20 mL methanol and 60 mL water	UV-LEDs	3056 μmol h^{-1} g^{-1}	12.4%	101
6	0.38 mol $Ni(OH)_2$/TiO_2	Pyrex flask, focused intensity: ~ 80 mW/cm^2, 20 mL methanol and 60 mL water	UV-LEDs	2273 μmol h^{-1} g^{-1}	9.3%	101
7	0.60 mol $Ni(OH)_2$/TiO_2	Pyrex flask, focused intensity: ca. 80 mW/cm^2, 20 mL methanol and 60 mL water	UV-LEDs	1804 μmol h^{-1} g^{-1}	7.3%	101
8	TiO_2/MoS_2/graphene	focused intensity 20 mW/cm^{-2}	350 W Xe arc lamp	165.3 μmol h^{-1}	9.7%	102
9	F-TiO_2 sphere with 45% {001} facets	80 mL water + 20 mL methanol	300 W Xe arc lamp	5841 μmol h^{-1} g-1	N.D.	103
10	50 wt % TiO_2 @MoS_2	quartz flask, 0.35 M Na_2S and 0.25 M Na_2SO_3	300 W xenon arc lamp	1.6 mmol h $^{-1}$ g $^{-1}$	N.D.	104
11	1.2 wt % Pt/TiO_2	quartz reactor, 54 mL water and 6 mL methanol	350 W mercury lamp	~2.7 mmol h^{-1} g^{-1}	N.D.	98
12	1 wt % Pt/TiO_2	10 vol % methanol solution, top-irradiation vessel connected to a glass-enclosed gas circulation system	unknown	~800 μmol h^{-1} g^{-1}	N.D.	36
13	1 wt % Pt/B-TiO_2	10 vol % methanol solution, top-irradiation vessel connected to a glass-enclosed gas circulation system	unknown	~200 μmol h^{-1} g^{-1}	N.D.	36
14	0.3 wt % Pt/TiO_2	2.17 M Na_2CO_3	400 W mercury lamp	1893.3 μmol h^{-1} g^{-1}	N.D.	105
15	0.9 wt % Pt/TiO_2	Pyrex Ñask, 2 M KBr, 6.5 mM $FeCl_2$	500 W mercury lamp	233.3 μmol h^{-1} g^{-1}	N.D.	106
16	TiO_2	1 M NaOH solution	100 W Hg lamp	~7.5 μmol h^{-1}	N.D.	107
17	eosin Y sensitized 1.0 wt % CuO/TiO_2	15% diethanol amine, H_2O	200 W halogen lamp with a cutoff filter (λ > 420 nm)	~530 μmol h^{-1} g^{-1}	5.1%	108
18	eosin Y sensitized 0.5 wt % Pt/N-TiO_2	80 mL riethanolamine	400 W Hg lamp with a cutoff filter (λ > 420 nm)	~800 μmol h^{-1} g^{-1}	N.D.	109
19	eosin Y-Fe^{3+} (1:1) − 1.0 wt % Pt/TiO_2	80 mL 0.79 mol/L TEA solution as sacrifice electron donors; pH 7.0; initially N_2-saturated	metal halide lamp (400 W) with a cut-off filter (λ > 420 nm)	2750 μmol h^{-1} g^{-1}	19.1	110
20	eosin Y sensitized 1.0 wt % Rh/TiO_2	70 mL, 15% DEA H_2O; DEA as sacrifice electron donors;	200 W halogen lamp with a cutoff filter (λ > 420 nm)	730 μmol h^{-1} g^{-1}	7.1	111
21	eosin Y sensitized 0.1 wt % Pt/TiO_2	250 mL, 15% DEA H_2O; DEA as sacrifice electron donors;	300 W Xe lamp with a cutoff filter (λ > 460 nm)	~216.7 μmol h^{-1} g^{-1}	10	112
22	merocyanine sensitized 1.0 wt % Pt/TiO_2	100 mL 95% AN-H_2O;acetonitrile, I anions as sacrifice electron donors	300 W Xe lamp with a cutoff filter (λ > 440 nm)	~340 μmol h^{-1} g^{-1}	2	113
23	carboxylate, phosphonate in Ru complex-3.0 wt % Pt/TiO_2	EDTA as sacrifice electron donors	450 W Xe lamp with a cutoff filter (λ > 420 nm)	~8800 μmol h^{-1} g^{-1}	22.4	114
24	0.5 wt % Pt/TiO_2	75 mL of aqueous methanol solution	N.D. UV−visible light	~4266 μmol h^{-1} g^{-1}	N.D.	87

[a]Not determined.

catalyst. Photocatalysis on TiO_2 microsphere involves three main steps:[14,35,36,89] (i) when the energy of a photon is greater than the bandgap of the material, the photon is absorbed by the material and excites an electron from the valence band into the conduction band, leading to the generation of electron (e^-) and hole (h^+) pairs in the semiconductor particles; the properties of porous structure, large surface area and well crystallinity of TiO_2 microsphere will increase the size of the accessible surface area and the rate of mass transfer for visible or UV−visible light adsorption. (ii) Charge separation and the followed migration of these photogenerated carriers in TiO_2 nanoparticles, where the multiple scattering and reflections of light within the TiO_2 spheres would extend the light path length and reduce the recombination of electron and holes. (iii) Surface chemical reactions between these carriers with various compounds (e.g., H_2O); electrons and holes may also recombine with each other without participating in any chemical reactions. When the TiO_2 micropshere-derived photocatalyst is used for water splitting, the bottom of the conduction band must be more negative than the reduction potential (0 V vs NHE) of water to produce H_2.[90−94] The band structure, charge separation, and lifetime of photogenerated electrons and holes affect the photocatalytic generation of H_2 from water splitting significantly.

Recent Advances. A wide range of TiO_2 microsphere-derived materials have been developed as photocatalysts for use under UV−visible or visible light irradiation. These typical examples are shown in Table 3. After excited charges are created, charge recombination and separation are two important competitive processes inside the TiO_2 microsphere-derived photocatalysts that largely affect the efficiency of the photocatalytic reaction for water splitting.[95] It should be noted that crystal structure, crystallinity and particle size all strongly affect this step. Typically, the higher crystalline quality, the higher the activity toward photocatalytic water splitting because less defect sites, such as dislocation and grain

DOI: 10.1021/acssuschemeng.5b00154
ACS Sustainable Chem. Eng. 2015, 3, 779−791

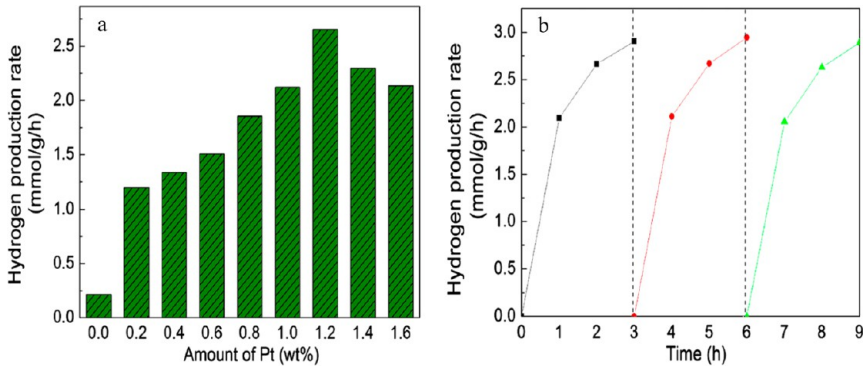

Figure 12. (a) Hydrogen generation rate of Pt loaded TiO_2 microspheres with different Pt loading amounts. (b) Time courses of photocatalytic H_2 production over the 1.2 wt % Pt/TiO_2 microspheres. Reprinted with permission.[98] Copyright 2013, Elsevier.

boundaries, exist to promote the recombination of electron hole pairs.[96,97]

Wei et al.[98] reported the synthesis of TiO_2 microspheres using a template-free method in the presence of hydrofluoric acid and titanium butanoxide as the precursor. The different amounts (0.1−1.6 wt %) of Pt supported on TiO_2 microspheres were prepared by the impregnation-reduction method. The H_2 evolution rate as a function of Pt loading is shown in Figure 12a. The optimal amount of cocatalyst Pt loading was 1.2 wt % and presented the H_2 evolution rate of ∼3.0 mmol h^{-1} g^{-1}. The high activity was due to the enhanced visible absorption and the presence of cocatalyst Pt. The good crystallinity, small and relatively homogeneous distribution of particle, and large surface area would contribute significantly for the light adsorption. The presence of cocatalyst Pt could act as better traps for photogenerated electrons in the interior of the TiO_2 microsphere and efficient separation of photoinduced electrons and holes. The life stability is another crucial parameter to realize the practical applications. The repeatability on the 1.2 wt % Pt/TiO_2 microsphere was tested over three cycles, as shown in Figure 12b. No degradation was found, which confirmed a high stability of the resulted TiO_2 microsphere.

Dinh et al.[51] reported the construction of three-dimensional ordered assembly of thin-shell Au/TiO_2 hollow nanospheres, where the TiO_2 hollow nanospheres were fabricated in the presence of soft template oleylamine using a titanium butoxide precursor. The designed photocatalyst exhibited not only exceedingly high surface area but also photonic behavior originating from periodic macroscopic voids from both the inside and the outside of hollow spheres that have very thin shells. The multiple light scattering and slow photon effects resulting from this unique architecture greatly enhanced the surface plasmon resonance of Au nanoparticles, which leaded to a significant enhancement in the visible light absorption. As a result, these new photocatalysts exhibited a photocatalytic activity that was several times higher than conventional Au/TiO_2 nanopowders under visible-light illumination.

Liu et al.[34] have synthesized mesoporous brown carbonate-doped TiO_2 microspheres with a combination of features by a template-free method using a titanium isopropoxide precursor. These features contributed the high photocatalytic activity that included the high specific surface area, tunable pore diameter and grain size, high crystallinity, well-defined morphology, and high visible light absorption due to carbonate doping. By adjusting the amount of titanium alkoxide in the starting reaction solution and the solvothermal reaction time, the microsphere diameter, nanocrystallite size, pore diameter, and specific surface area could be varied. The as-prepared carbonate-doped TiO_2 microspheres display remarkable performance with the H_2 production rate of ∼200 μmol h^{-1} g^{-1}, which were 3 orders of magnitude more photoactive than commercial TiO_2 nanoparticles under visible light illumination. This method is convenient and easy to scale-up, which is highly promising for H_2 production.

Overall, TiO_2 microspheres not only share common characteristics with nanoparticles but also offer unique properties that are difficult to achieve in nanoparticles. The good crystallinity, high specific surface area, tunable pore volume and pore size, well-defined morphology, and easy doping would enhance the mass transfer for visible or UV−visible light adsorption and increase the light-harvesting capabilities. The hollow interior and porous structure would trap more photons, enhance the photogenerated charge separation, and reduce the recombination of electrons and holes.

CONCLUSIONS

The synthesis of TiO_2 microsphere-derived photocatalysts has had increased attention over the past few decades and will likely continue to increase in the coming years. These TiO_2 microsphere-derived materials offer unique properties (e.g., large surface area, better mass transfer for visible light adsorption, trapping more photons, the reduced recombination of electron and holes). With these properties, enhanced photocatalytic activities of H_2 production on TiO_2 microsphere-derived photocatalysts have been achieved. With the increasing need for clean and sustainable H_2 energy sources, TiO_2 microsphere-derived materials may play a crucial role in developing solutions to many of these problems.

A templated method has been proved to be an effective strategy to yield TiO_2 microspheres with specific functionality. Although many template syntheses are labor and energy intensive, much recent progress has been made. Through the careful control of the self-assembly, titanium condensation rate, and other parameters, it is possible to change the dimensions, crystal structures, and morphologies of TiO_2 microspheres. Due to the low cost and simple operation, the one-step template-free method has great promise for the controlled preparation of hollow structures in a wide range of sizes. The crystallinity, crystal structure, surface structure, and morphology need to be investigated systematically in the synthesis and further modified to optimize the preparation method.

DOI: 10.1021/acssuschemeng.5b00154
ACS Sustainable Chem. Eng. 2015, 3, 779−791

A number of modification techniques and chemical additives have been developed in recent years to improve photocatalytic H_2 production from water splitting on TiO_2 microsphere-derived photocatalysts under UV and visible light irradiation. Due to the quick charge recombination of electrons and produced holes, fast backward reaction, and poor ability in the utilization of visible light, the H_2 evolution rate reported is low and there is still large room for improvement.

Because this perspective does not involve the theoretical calculation, future studies on computational prediction based on first-principle, or density functional theory calculations, it may provide an efficient way to identify TiO_2 microspheres with specific morphologies and suggest useful processing and production conditions. Additionally, new insights are needed into the water-splitting mechanism, particularly with regards to identification of any thermodynamic and kinetic bottlenecks. This would facilitate the design of the most effective photocatalytic water-splitting systems.

AUTHOR INFORMATION

Corresponding Authors

*G. Wu. Tel.: 609 224 3103. E-mail: gwu@lakeheadu.ca.
*K. Yan. Tel.: 609 224 3103. E-mail: kai_yan@brown.edu.

Notes

The authors declare no competing financial interest.

Biographies

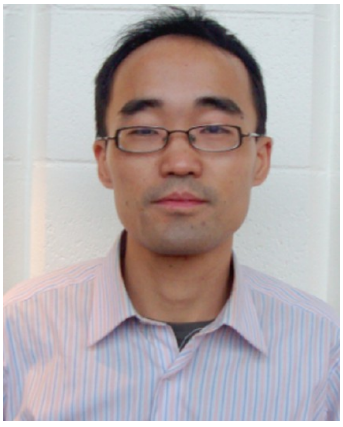

Kai Yan is currently working in the School of Engineering at Brown University as a postdoctoral research associate. He started his Ph.D. study at the Max-Planck-Institute for Coal Research in 2008 in Germany with the support of Max-Planck-Society Scholarship. He obtained his Ph.D. from RWTH Aachen University in 2011. He obtained an Ontario Postdoctoral Fellowship in 2012. His research interests concentrate on the development of robust nanomaterials for catalytic conversion of biomass-derived monomers into fuel as well as value-added chemicals, photocatalysis, and electrocatalysis for energy generation. Currently, he is the author and coauthor of 30 journal papers and a book chapter, publishing mainly in the area of sustainable energy generation.

Guosheng Wu completed his Ph.D. at the Institute of Solid State Physics, Chinese Academy of Sciences in 2004. After obtaining his Ph.D. in 2004, he was an assistant professor at Anhui University, China, and then he moved to Lakehead University (Canada) as a postdoctoral fellow, he is now a materials scientist at the Department of Chemistry and Instrumentation Laboratory, Lakehead University. His main research interests are the design of earth abundant, high efficient photocatalysts for environmental purification and solar to fuel conversion. He is the author and coauthor of more than 50 peer-reviewed papers and a book chapter.

REFERENCES

(1) Linsebigler, A. L.; Lu, G.; Yates, J. T., Jr. Photocatalysis on TiO_2 surfaces: Principles, mechanisms, and selected results. *Chem. Rev.* **1995**, *95*, 735−758.
(2) Ma, Y.; Wang, X.; Jia, Y.; Chen, X.; Han, H.; Li, C. Titanium dioxide-based nanomaterials for photocatalytic fuel generations. *Chem. Rev.* **2014**, *114*, 9987−10043.
(3) Ardo, S.; Achey, D.; Morris, A. J.; Abrahamsson, M.; Meyer, G. J. Non-Nernstian two-electron transfer photocatalysis at metalloporphyrin−TiO_2 interfaces. *J. Am. Chem. Soc.* **2011**, *133*, 16572−16580.
(4) Bachmeier, A.; Wang, V. C. C.; Woolerton, T. W.; Bell, S.; Fontecilla-Camps, J. C.; Can, M.; Ragsdale, S. W.; Chaudhary, Y. S.; Armstrong, F. A. How light-harvesting semiconductors can alter the bias of reversible electrocatalysts in favor of H_2 production and CO_2 reduction. *J. Am. Chem. Soc.* **2013**, *135*, 15026−15032.
(5) Yeh, S. C.; Lee, P. H.; Liao, H. Y.; Chen, Y. Y.; Chen, C. T.; Jeng, R. J.; Shuye, J. J. Facile solution dropping method: A green process for dyeing TiO_2 electrodes of dye-sensitized solar cells with enhanced power conversion efficiency. *ACS Sustainable Chem. Eng.* **2014**, 3, 71−81.
(6) Maeda, K.; Domen, K. Photocatalytic water splitting: Recent progress and future challenges. *J. Phys. Chem. Lett.* **2010**, *1*, 2655−2661.
(7) Xu, M.; Ruan, P.; Xie, H.; Yu, A.; Zhou, X. Mesoporous TiO_2 single-crystal polyhedron-constructed core−shell microspheres: Anisotropic etching and photovoltaic property. *ACS Sustainable Chem. Eng.* **2014**, *2*, 621−628.
(8) Liu, C. J.; Burghaus, U.; Besenbacher, F.; Wang, Z. L. Preparation and characterization of nanomaterials for sustainable energy production. *ACS Nano* **2010**, *4*, 5517−5526.
(9) Protti, S.; Albini, A.; Serpone, N. Photocatalytic generation of solar fuels from the reduction of H_2O and CO_2: A look at the patent literature. *Phys. Chem. Chem. Phys.* **2014**, *16*, 19790−19827.
(10) Shen, S.; Shi, J.; Guo, P.; Guo, L. Visible-light-driven photocatalytic water splitting on nanostructured semiconducting materials. *Int. J. Nanotechnol.* **2011**, *8*, 523−591.
(11) Wu, G.; Thind, S. S.; Wen, J.; Yan, K.; Chen, A. A novel nanoporous α-C_3N_4 photocatalyst with superior high visible light activity. *Appl. Catal., B* **2013**, *142*−*143*, 590−597.
(12) Fujishima, A.; Honda, K. Electrochemical photolysis of water at a semiconductor electrode. *Nature* **1972**, *238*, 37−38.

DOI: 10.1021/acssuschemeng.5b00154
ACS Sustainable Chem. Eng. 2015, 3, 779−791

(13) Deepak, T. G.; Subash, D.; Anjusree, G. S.; Pai, K. N.; Nair, S. V.; Nair, A. S. Photovoltaic property of anatase TiO_2 3-D mesoflowers. *ACS Sustainable Chem. Eng.* **2014**, *2*, 2772−2780.
(14) Tsui, L. K.; Huang, J.; Sabat, M.; Zangari, G. Visible light sensitization of TiO_2 nanotubes by bacteriochlorophyll-c dyes for photoelectrochemical solar cells. *ACS Sustainable Chem. Eng.* **2014**, *2*, 2097−2101.
(15) Wu, G.; Wang, J.; Thomas, D. F.; Chen, A. Synthesis of F-doped flower-like TiO_2 nanostructures with high photoelectrochemical activity. *Langmuir* **2008**, *24*, 3503−3509.
(16) Li, B.; Gao, X.; Zhang, H. C.; Yuan, C. Energy modeling of electrochemical anodization process of titanium dioxide nanotubes. *ACS Sustainable Chem. Eng.* **2013**, *2*, 404−410.
(17) Wu, G.; Tian, M.; Chen, A. Synthesis of CdS quantum-dot sensitized TiO_2 nanowires with high photocatalytic activity for water splitting. *J. Photochem. Photobiol., A* **2012**, *233*, 65−71.
(18) Wu, G.; Wu, J. L.; Samantha, N.; Chen, A. One-step synthesis of N- and F-codoped mesoporous TiO_2 photocatalysts with high visible light activity. *Nanotechnol.* **2010**, *21*, 085701.
(19) Yan, K.; Wu, G.; Jarvis, C.; Wen, J.; Chen, A. Facile synthesis of porous microspheres composed of TiO_2 nanorods with high photocatalytic activity for hydrogen production. *Appl. Catal., B* **2014**, *148−149*, 281−287.
(20) Wu, G.; Nishikawa, T.; Ohtani, B.; Chen, A. Synthesis and characterization of carbon-doped TiO_2 nanostructures with enhanced visible light response. *Chem. Mater.* **2007**, *19*, 4530−4537.
(21) Murakami, N.; Prieto Mahaney, O. O.; Abe, R.; Torimoto, T.; Ohtani, B. Double-beam photoacoustic spectroscopic studies on transient absorption of titanium(IV) oxide photocatalyst powders. *J. Phys. Chem. C* **2007**, *111*, 11927−11935.
(22) Zhang, Q.; Joo, J. B.; Lu, Z.; Dahl, M.; Oliveira, D. Q.; Ye, M.; Yin, Y. Self-assembly and photocatalysis of mesoporous TiO_2 nanocrystal clusters. *Nano Res.* **2011**, *4*, 103−114.
(23) Parida, K. Facile fabrication of S-TiO_2/β-SiC nanocomposite photocatalyst for hydrogen evolution under visible light irradiation. *ACS Sustainable Chem. Eng.* **2015**, *3*, 245−253.
(24) Chen, Y.; Kanan, M. W. Tin oxide dependence of the CO_2 reduction efficiency on tin electrodes and enhanced activity for tin/tin oxide thin-film catalysts. *J. Am. Chem. Soc.* **2012**, *134*, 1986−1989.
(25) Kondratenko, E. V.; Mul, G.; Baltrusaitis, J.; Larrazabal, G. O.; Perez-Ramirez, J. Status and perspectives of CO_2 conversion into fuels and chemicals by catalytic, photocatalytic and electrocatalytic processes. *Energy Environ. Sci.* **2013**, *6*, 3112−3135.
(26) Wu, G.; Adams, B.; Tian, M.; Chen, A. Synthesis and electrochemical study of novel Pt-decorated Ti nanowires. *Electrochem. Commun.* **2009**, *11*, 736−739.
(27) Almaschio, C. J.; Leite, E. R. Detachment induced by rayleigh-instability in metal oxide nanorods: Insights from TiO_2. *Cryst. Growth Des.* **2012**, *12*, 3668−3674.
(28) Carp, O.; Huisman, C. L.; Reller, A. Photoinduced reactivity of titanium dioxide. *Prog. Solid State Chem.* **2004**, *32*, 33−177.
(29) Zhou, W.; Li, W.; Wang, J. Q.; Qu, Y.; Yang, Y.; Xie, Y.; Zhao, D. Ordered mesoporous black TiO_2 as highly efficient hydrogen evolution photocatalyst. *J. Am. Chem. Soc.* **2014**, *136*, 9280−9283.
(30) Shimura, K.; Yoshida, H. Heterogeneous photocatalytic hydrogen production from water and biomass derivatives. *Energy Environ. Sci.* **2011**, *4*, 2467−2481.
(31) Acar, C.; Dincer, I.; Zamfirescu, C. A review on selected heterogeneous photocatalysts for hydrogen production. *Int. J. Energy Res.* **2014**, *38*, 1903−1920.
(32) Wu, T. T.; Xie, Y. P.; Yin, L. C.; Liu, G.; Cheng, H. M. Switching photocatalytic H_2 and O_2 generation preferences of rutile TiO_2 microspheres with dominant reactive facets by boron doping. *J. Phys. Chem. C* **2015**, *119*, 84−89.
(33) Li, W.; Yang, J.; Wu, Z.; Wang, J.; Li, B.; Feng, S.; Deng, Y.; Zhang, F.; Zhao, D. A versatile kinetics-controlled coating method to construct uniform porous TiO_2 shells for multifunctional core−shell structures. *J. Am. Chem. Soc.* **2012**, *134*, 11864−11867.
(34) Liu, B.; Liu, L. M.; Lang, X. F.; Wang, H. Y.; Lou, X. W.; Aydil, E. S. Doping high-surface-area mesoporous TiO_2 microspheres with carbonate for visible light hydrogen production. *Energy Environ. Sci.* **2014**, *7*, 2592−2597.
(35) Bahruji, H.; Bowker, M.; Davies, P. R.; Pedrono, F. New insights into the mechanism of photocatalytic reforming on Pd/TiO_2. *Appl. Catal., B* **2011**, *107*, 205−209.
(36) Liu, G.; Pan, J.; Yin, L.; Irvine, J. T. S.; Li, F.; Tan, J.; Wormald, P.; Cheng, H. M. Heteroatom-modulated switching of photocatalytic hydrogen and oxygen evolution preferences of anatase TiO_2 microspheres. *Adv. Funct. Mater.* **2012**, *22*, 3233−3238.
(37) Schneider, J.; Matsuoka, M.; Takeuchi, M.; Zhang, J.; Horiuchi, Y.; Anpo, M.; Bahnemann, D. W. Understanding TiO_2 photocatalysis: Mechanisms and materials. *Chem. Rev.* **2014**, *114*, 9919−9986.
(38) Bai, Y.; Mora-Seró, I.; De Angelis, F.; Bisquert, J.; Wang, P. Titanium dioxide nanomaterials for photovoltaic applications. *Chem. Rev.* **2014**, *114*, 10095−10130.
(39) Fujishima, A.; Zhang, X.; Tryk, D. A. TiO_2 photocatalysis and related surface phenomena. *Surf. Sci. Rep.* **2008**, *63*, 515−582.
(40) Dahl, M.; Liu, Y.; Yin, Y. Composite titanium dioxide nanomaterials. *Chem. Rev.* **2014**, *114*, 9853−9889.
(41) Reynal, A.; Lakadamyali, F.; Gross, M. A.; Reisner, E.; Durrant, J. R. Parameters affecting electron transfer dynamics from semiconductors to molecular catalysts for the photochemical reduction of protons. *Energy Environ. Sci.* **2013**, *6*, 3291−3300.
(42) Asahi, R.; Morikawa, T.; Irie, H.; Ohwaki, T. Nitrogen-doped titanium dioxide as visible-light-sensitive photocatalyst: Designs, developments, and prospects. *Chem. Rev.* **2014**, *114*, 9824−9852.
(43) Lou, X. W.; Archer, L. A.; Yang, Z. Hollow micro-/nanostructures: Synthesis and applications. *Adv. Mater.* **2008**, *20*, 3987−4019.
(44) Zhu, F.; Wu, D.; Li, Q.; Dong, H.; Li, J.; Jiang, K.; Xu, D. Hierarchical TiO_2 microspheres: Synthesis, structural control and their applications in dye-sensitized solar cells. *RSC Adv.* **2012**, 11629−11637.
(45) Hu, Y.; Ge, J.; Sun, Y.; Zhang, T.; Yin, Y. A self-templated approach to TiO_2 microcapsules. *Nano Lett.* **2007**, *7*, 1832−1836.
(46) Cui, Y.; Liu, L.; Li, B.; Zhou, X.; Xu, N. Fabrication of tunable core−shell structured TiO_2 mesoporous microspheres using linear polymer polyethylene glycol as templates. *J. Phys. Chem. C* **2010**, *114*, 2434−2439.
(47) Jiao, Y.; Peng, C.; Guo, F.; Bao, Z.; Yang, J.; Schmidt-Mende, L.; Dunbar, R.; Qin, Y.; Deng, Z. Facile synthesis and photocatalysis of size-distributed TiO_2 hollow spheres consisting of {116} plane-oriented nanocrystallites. *J. Phys. Chem. C* **2011**, *115*, 6405−6409.
(48) Ding, S.; Huang, F.; Mou, X.; Wu, J.; Lu, X. Mesoporous hollow TiO_2 microspheres with enhanced photoluminescence prepared by a smart amino acid template. *J. Mater. Chem.* **2011**, *21*, 4888−4892.
(49) Wu, X.; Lu, G. Q.; Wang, L. Shell-in-shell TiO_2 hollow spheres synthesized by one-pot hydrothermal method for dye-sensitized solar cell application. *Energy Environ. Sci.* **2011**, *4*, 3565−3572.
(50) Yu, J.; Zhang, J. A simple template-free approach to TiO_2 hollow spheres with enhanced photocatalytic activity. *Dalton Trans.* **2010**, *39*, 5860−5867.
(51) Dinh, C. T.; Yen, H.; Kleitz, F.; Do, T. O. Three-dimensional ordered assembly of thin-shell Au/TiO_2 hollow nanospheres for enhanced visible-light-driven photocatalysis. *Angew. Chem., Int. Ed.* **2014**, *53*, 6618−6623.
(52) Dong, Y.; Wang, Y.; Cai, T.; Kou, L.; Yang, G.; Yan, Z. Preparation and nitrogen-doping of three-dimensionally ordered macroporous TiO_2 with enhanced photocatalytic activity. *Ceram. Int.* **2014**, *40*, 11213−11219.
(53) Kondo, Y.; Yoshikawa, H.; Awaga, K.; Murayama, M.; Mori, T.; Sunada, K.; Bandow, S.; Iijima, S. Preparation, photocatalytic activities, and dye-sensitized solar-cell performance of submicron-scale TiO_2 hollow spheres. *Langmuir* **2007**, *24*, 547−550.
(54) Yang, Z.; Niu, Z.; Lu, Y.; Hu, Z.; Han, C. C. Templated synthesis of inorganic hollow spheres with a tunable cavity size onto core−shell gel particles. *Angew. Chem., Int. Ed.* **2003**, *42*, 1943−1945.

DOI: 10.1021/acssuschemeng.5b00154
ACS Sustainable Chem. Eng. 2015, 3, 779−791

(55) Li, X.; Xiong, Y.; Li, Z.; Xie, Y. Large-scale fabrication of TiO_2 hierarchical hollow spheres. *Inorg. Chem.* **2006**, *45*, 3493−3495.
(56) Shang, S.; Jiao, X.; Chen, D. Template-free fabrication of TiO_2 hollow spheres and their photocatalytic properties. *ACS Appl. Mater. Interface* **2011**, *4*, 860−865.
(57) He, Z.; Liu, J.; Miao, J.; Liu, B.; Yang Tan, T. T. A one-pot solvothermal synthesis of hierarchical microspheres with radially assembled single-crystalline TiO_2-nanorods for high performance dye-sensitized solar cells. *J. Mater. Chem. C* **2014**, *2*, 1381−1385.
(58) Matijević, E.; Budnik, M.; Meites, L. Preparation and mechanism of formation of titanium dioxide hydrosols of narrow size distribution. *J. Colloid Interface Sci.* **1977**, *61*, 302−311.
(59) Niederberger, M.; Bartl, M. H.; Stucky, G. D. Benzyl alcohol and transition metal chlorides as a versatile reaction system for the nonaqueous and low-temperature synthesis of crystalline nano-objects with controlled dimensionality. *J. Am. Chem. Soc.* **2002**, *124*, 13642−13643.
(60) Barringer, E. A.; Bowen, H. K. Formation, packing, and sintering of monodisperse TiO_2 powders of monodisperse TiO_2 powders. *J. Am. Ceram. Soc.* **1982**, *65*, C-199−C-201.
(61) Zheng, Z.; Huang, B.; Qin, X.; Zhang, X.; Dai, Y. Strategic synthesis of hierarchical TiO_2 microspheres with enhanced photocatalytic activity. *Chem.—Eur. J.* **2010**, *16*, 11266−11270.
(62) Liu, S.; Yu, J.; Jaroniec, M. Tunable photocatalytic selectivity of hollow TiO_2 microspheres composed of anatase polyhedra with exposed {001} facets. *J. Am. Chem. Soc.* **2010**, *132*, 11914−11916.
(63) Li, H.; Bian, Z.; Zhu, J.; Zhang, D.; Li, G.; Huo, Y.; Li, H.; Lu, Y. Mesoporous titania spheres with tunable chamber stucture and enhanced photocatalytic activity. *J. Am. Chem. Soc.* **2007**, *129*, 8406−8407.
(64) Yan, K.; Lafleur, T.; Liao, J.; Xie, X. Facile green synthesis of palladium nanoparticles for efficient liquid-phase hydrogenation of biomass-derived furfural. *Sci. Adv. Mater.* **2014**, *6*, 135−140.
(65) Yan, K.; Wu, X.; An, X.; Xie, X. Novel preparation of nanocomposite CuO-Cr_2O_3 Using CTAB-template method and efficient for hydrogenation of biomass-derived furfural. *Funct. Mater. Lett.* **2013**, *6*, 1350007.
(66) Liu, Y.; Goebl, J.; Yin, Y. Templated synthesis of nanostructured materials. *Chem. Soc. Rev.* **2013**, *42*, 2610−2653.
(67) Yan, K.; Lafleur, T.; Jarvis, C.; Wu, G. Clean and selective production of γ-valerolactone from biomass-derived levulinic acid catalyzed by recyclable Pd nanoparticle catalyst. *J. Clean. Prod.* **2014**, *72*, 230−232.
(68) Yan, K.; Wu, G.; Wen, J.; Chen, A. One-step synthesis of mesoporous $H_4SiW_{12}O_{40}$-SiO_2 catalysts for the production of methyl and ethyl levulinate biodiesel. *Catal. Commun.* **2013**, *34*, 58−63.
(69) Gu, D.; Schuth, F. Synthesis of non-siliceous mesoporous oxides. *Chem. Soc. Rev.* **2014**, *43*, 313−344.
(70) Qian, J.; Liu, P.; Xiao, Y.; Jiang, Y.; Cao, Y.; Ai, X.; Yang, H. TiO_2-coated multilayered SnO_2 hollow microspheres for dye-sensitized solar cells. *Adv. Mater.* **2009**, *21*, 3663−3667.
(71) Ren, Y.; Ma, Z.; Bruce, P. G. Ordered mesoporous metal oxides: Synthesis and applications. *Chem. Soc. Rev.* **2012**, *41*, 4909−4927.
(72) Caruso, F.; Caruso, R. A.; Möhwald, H. Nanoengineering of inorganic and hybrid hollow spheres by colloidal templating. *Science* **1998**, *282*, 1111−1114.
(73) Lu, A. H.; Schüth, F. Nanocasting: A versatile strategy for creating nanostructured porous materials. *Adv. Mater.* **2006**, *18*, 1793−1805.
(74) Ren, H.; Yu, R.; Wang, J.; Jin, Q.; Yang, M.; Mao, D.; Wang, D. Multishelled TiO_2 hollow microspheres as anodes with superior reversible capacity for lithium ion batteries. *Nano Lett.* **2014**, *14*, 6679−6684.
(75) Yang, M.; Ma, J.; Zhang, C.; Yang, Z.; Lu, Y. General synthetic route toward functional hollow spheres with double-shelled structures. *Angew. Chem., Int. Ed.* **2005**, *44*, 6727−6730.
(76) Song, X.; Gao, L. Synthesis, characterization, and optical properties of well-defined N-doped, hollow silica/titania hybrid microspheres. *Langmuir* **2007**, *23*, 11850−11856.
(77) Shin, S. S.; Kim, D. W.; Park, J. H.; Kim, D. H.; Kim, J. S.; Hong, K. S.; Cho, I. S. Anionic ligand assisted synthesis of 3-D hollow TiO_2 architecture with enhanced photoelectrochemical performance. *Langmuir* **2014**, *30*, 15531−15539.
(78) Asahi, R.; Morikawa, T.; Ohwaki, T.; Aoki, K.; Taga, Y. Visible-light photocatalysis in nitrogen-doped titanium oxides. *Science* **2001**, *293*, 269−271.
(79) Xuan, S.; Jiang, W.; Gong, X.; Hu, Y.; Chen, Z. Magnetically separable Fe_3O_4/TiO_2 hollow spheres: Fabrication and photocatalytic activity. *J. Phys. Chem. C* **2008**, *113*, 553−558.
(80) Kapilashrami, M.; Zhang, Y.; Liu, Y. S.; Hagfeldt, A.; Guo, J. Probing the optical property and electronic structure of TiO_2 nanomaterials for renewable energy applications. *Chem. Rev.* **2014**, *114*, 9662−9707.
(81) Lou, X. W.; Archer, L. A. A general route to nonspherical anatase TiO_2 hollow colloids and magnetic multifunctional particles. *Adv. Mater.* **2008**, *20*, 1853−1858.
(82) Jin, Z.; Wang, F.; Wang, F.; Wang, J.; Yu, J. C.; Wang, J. Metal nanocrystal-embedded hollow mesoporous TiO_2 and ZrO_2 microspheres prepared with polystyrene nanospheres as carriers and templates. *Adv. Funct. Mater.* **2013**, *23*, 2137−2144.
(83) Liu, B.; Nakata, K.; Sakai, M.; Saito, H.; Ochiai, T.; Murakami, T.; Takagi, K.; Fujishima, A. Mesoporous TiO_2 core−shell spheres composed of nanocrystals with exposed high-energy facets: facile synthesis and formation mechanism. *Langmuir* **2011**, *27*, 8500−8508.
(84) Suteewong, T.; Sai, H.; Hovden, R.; Muller, D.; Bradbury, M. S.; Gruner, S. M.; Wiesner, U. Multicompartment mesoporous silica nanoparticles with branched shapes: an epitaxial growth mechanism. *Science* **2013**, *340*, 337−341.
(85) Kudo, A.; Miseki, Y. Heterogeneous photocatalyst materials for water splitting. *Chem. Soc. Rev.* **2009**, *38*, 253−278.
(86) Sheng, H.; Ji, H.; Ma, W.; Chen, C.; Zhao, J. Direct four-electron reduction of O_2 to H_2O on TiO_2 surfaces by pendant proton relay. *Angew. Chem., Int. Ed.* **2013**, *52*, 9686−9690.
(87) Kandiel, T. A.; Feldhoff, A.; Robben, L.; Dillert, R.; Bahnemann, D. W. Tailored titanium dioxide nanomaterials: Anatase nanoparticles and brookite nanorods as highly active photocatalysts. *Chem. Mater.* **2010**, *22*, 2050−2060.
(88) Wang, H.; Miyauchi, M.; Ishikawa, Y.; Pyatenko, A.; Koshizaki, N.; Li, Y.; Li, L.; Li, X.; Bando, Y.; Golberg, D. Single-crystalline rutile TiO_2 hollow spheres: room-temperature synthesis, tailored visible-light-extinction, and effective scattering layer for quantum dot-sensitized solar cells. *J. Am. Chem. Soc.* **2011**, *133*, 19102−19109.
(89) Khan, S. U. M.; Al-Shahry, M.; Ingler, W. B. Efficient photochemical water splitting by a chemically modified n-TiO_2. *Science* **2002**, *297*, 2243−2245.
(90) Kisch, H. Semiconductor photocatalysis—Mechanistic and synthetic aspects. *Angew. Chem., Int. Ed.* **2013**, *52*, 812−847.
(91) Hisatomi, T.; Kubota, J.; Domen, K. Recent advances in semiconductors for photocatalytic and photoelectrochemical water splitting. *Chem. Soc. Rev.* **2014**, *43*, 7520−7535.
(92) Abe, R.; Sayama, K.; Sugihara, H. Development of new photocatalytic water splitting into H_2 and O_2 using two different semiconductor photocatalysts and a shuttle redox mediator IO_3^-/I^-. *J. Phys. Chem. B* **2005**, *109*, 16052−16061.
(93) Sayama, K.; Yoshida, R.; Kusama, H.; Okabe, K.; Abe, Y.; Arakawa, H. Photocatalytic decomposition of water into H_2 and O_2 by a two-step photoexcitation reaction using a WO_3 suspension catalyst and an Fe^{3+}/Fe^{2+} redox system. *Chem. Phys. Lett.* **1997**, *277*, 387−391.
(94) Maeda, K.; Domen, K. New non-oxide photocatalysts designed for overall water splitting under visible light. *J. Phys. Chem. C* **2007**, *111*, 7851−7861.
(95) Kudo, A.; Miseki, Y. Heterogeneous photocatalyst materials for water splitting. *Chem. Soc. Rev.* **2009**, *38*, 253−278.
(96) Ni, M.; Leung, M. K. H.; Leung, D. Y. C.; Sumathy, K. A review and recent developments in photocatalytic water-splitting using for hydrogen production. *Renewable Sustainable Energy Rev.* **2007**, *11*, 401−425.

DOI: 10.1021/acssuschemeng.5b00154
ACS Sustainable Chem. Eng. 2015, 3, 779−791

(97) Li, F. B.; Li, X. Z. The enhancement of photodegradation efficiency using Pt−TiO_2 catalyst. *Chemosphere* **2002**, *48*, 1103−1111.
(98) Wei, P.; Liu, J.; Li, Z. Effect of Pt loading and calcination temperature on the photocatalytic hydrogen production activity of TiO_2 microspheres. *Ceram. Int.* **2013**, *39*, 5387−5391.
(99) Li, H.; Zhang, X.; Cui, X. A facile and waste-free strategy to fabricate Pt-C/TiO_2 microspheres: Enhanced photocatalytic performance for hydrogen evolution. *Int. J. Photoenergy* **2014**, *2014*.
(100) Yu, J.; Qi, L.; Jaroniec, M. Hydrogen production by photocatalytic water splitting over Pt/TiO_2 nanosheets with exposed (001) facets. *J. Phys. Chem. C* **2010**, *114*, 13118−13125.
(101) Yu, J.; Hai, Y.; Cheng, B. Enhanced photocatalytic H_2-production activity of TiO_2 by $Ni(OH)_2$ cluster modification. *J. Phys. Chem. C* **2011**, *115*, 4953−4958.
(102) Xiang, Q.; Yu, J.; Jaroniec, M. Synergetic effect of MoS_2 and graphene as cocatalysts for enhanced photocatalytic H_2 production activity of TiO_2 nanoparticles. *J. Am. Chem. Soc.* **2012**, *134*, 6575−6578.
(103) Zheng, Z.; Huang, B.; Lu, J.; Qin, X.; Zhang, X.; Dai, Y. Hierarchical TiO_2 microspheres: synergetic effect of {001} and {101} facets for enhanced photocatalytic activity. *Chem.—Eur. J.* **2011**, *17*, 15032−15038.
(104) Zhou, W.; Yin, Z.; Du, Y.; Huang, X.; Zeng, Z.; Fan, Z.; Liu, H.; Wang, J.; Zhang, H. Synthesis of few-layer MoS_2 nanosheet-coated TiO_2 nanobelt heterostructures for enhanced photocatalytic activities. *Small* **2013**, *9*, 140−147.
(105) Sayama, K.; Arakawa, H. Effect of carbonate salt addition on the photocatalytic decomposition of liquid water over Pt-TiO_2 catalyst. *J. Chem. Soc. Faraday Trans.* **1997**, *93*, 1647−1654.
(106) Fujihara, K.; Ohno, T.; Matsumura, M. Splitting of water by electrochemical combination of two photocatalytic reactions on TiO_2 particles. *J. Chem. Soc., Faraday Trans.* **1998**, *94*, 3705−3709.
(107) Huang, C. W.; Liao, C. H.; Wu, J. C. S.; Liu, Y. C.; Chang, C. L.; Wu, C. H.; Anpo, M.; Matsuoka, M.; Takeuchi, M. Hydrogen generation from photocatalytic water splitting over TiO_2 thin film prepared by electron beam-induced deposition. *Int. J. Hydrogen Energy* **2010**, *35*, 12005−12010.
(108) Jin, Z.; Zhang, X.; Li, Y.; Li, S.; Lu, G. 5.1% Apparent quantum efficiency for stable hydrogen generation over eosin-sensitized CuO/TiO_2 photocatalyst under visible light irradiation. *Catal. Commun.* **2007**, *8*, 1267−1273.
(109) Li, Y.; Xie, C.; Peng, S.; Lu, G.; Li, S. Eosin Y-sensitized nitrogen-doped TiO_2 for efficient visible light photocatalytic hydrogen evolution. *J. Mol. Catal. A* **2008**, *282*, 117−123.
(110) Li, Y.; Guo, M.; Peng, S.; Lu, G.; Li, S. Formation of multilayer-Eosin Y-sensitized TiO_2 via Fe^{3+} coupling for efficient visible-light photocatalytic hydrogen evolution. *Int. J. Hydrogen Energy* **2009**, *34*, 5629−5636.
(111) Jin, Z.; Zhang, X.; Lu, G.; Li, S. Improved quantum yield for photocatalytic hydrogen generation under visible light irradiation over eosin sensitized TiO_2—Investigation of different noble metal loading. *J. Mol. Catal. A: Chem.* **2006**, *259*, 275−280.
(112) Abe, R.; Hara, K.; Sayama, K.; Domen, K.; Arakawa, H. Steady hydrogen evolution from water on Eosin Y-fixed TiO_2 photocatalyst using a silane-coupling reagent under visible light irradiation. *J. Photochem. Photobiol., A* **2000**, *137*, 63−69.
(113) Abe, R.; Sayama, K.; Arakawa, H. Efficient hydrogen evolution from aqueous mixture of I^- and acetonitrile using a merocyanine dye-sensitized Pt/TiO_2 photocatalyst under visible light irradiation. *Chem. Phys. Lett.* **2002**, *362*, 441−444.
(114) Bae, E.; Choi, W. Effect of the anchoring group (carboxylate vs phosphonate) in Ru-complex-sensitized TiO_2 on hydrogen production under visible light. *J. Phys. Chem. B* **2006**, *110*, 14792−14799.

DOI: 10.1021/acssuschemeng.5b00154
ACS Sustainable Chem. Eng. 2015, 3, 779−791